

Vertical Distribution and Diversity of Phototrophic Bacteria within a Hot Spring Microbial Mat (Nakabusa Hot Springs, Japan)

JOVAL N. MARTINEZ^{1,2}, ARISA NISHIHARA^{1,3}, MADIS LICHTENBERG⁴, ERIK TRAMPE⁴, SHIGERU KAWAI¹, MARCUS TANK¹, MICHAEL KÜHL⁴, SATOSHI HANADA¹, and VERA THIEL^{1*}

¹Department of Biological Sciences, Graduate School of Science, Tokyo Metropolitan University, 1–1 Minami-Osawa, Hachioji, Tokyo 192–0397, Japan; ²Department of Natural Sciences, College of Arts and Sciences, University of St. La Salle, Bacolod City, 6100 Negros Occidental, Philippines; ³Bioproduction Research Institute, National Institute of Advanced Industrial Science and Technology (AIST), Tsukuba, Ibaraki, Japan; and ⁴Marine Biological Section, Department of Biology, University of Copenhagen, Strandpromenaden 5, DK-3000 Helsingør, Denmark

(Received March 25, 2019—Accepted August 10, 2019—Published online November 2, 2019)

Phototrophic microbial mats are assemblages of vertically layered microbial populations dominated by photosynthetic microorganisms. In order to elucidate the vertical distribution and diversity of phototrophic microorganisms in a hot spring-associated microbial mat in Nakabusa (Japan), we analyzed the 16S rRNA gene amplicon sequences of the microbial mat separated into five depth horizons, and correlated them with microsensor measurements of O₂ and spectral scalar irradiance. A stable core community and high diversity of phototrophic organisms dominated by the filamentous anoxygenic phototrophs, *Roseiflexus castenholzii* and *Chloroflexus aggregans* were identified together with the spectral signatures of bacteriochlorophylls (BChls) *a* and *c* absorption in all mat layers. In the upper mat layers, a high abundance of cyanobacteria (*Thermosynechococcus* sp.) correlated with strong spectral signatures of chlorophyll *a* and phycobiliprotein absorption near the surface in a zone of high O₂ concentrations during the day. Deeper mat layers were dominated by uncultured chemotrophic *Chlorobi* such as the novel putatively sulfate-reducing “*Ca. Thermonerobacter* sp.”, which showed increasing abundance with depth correlating with low O₂ in these layers enabling anaerobic metabolism. Oxygen tolerance and requirements for the novel phototroph “*Ca. Chloroanaerofilum* sp.” and the uncultured chemotrophic *Armatimonadetes* member type OS-L detected in Nakabusa hot springs, Japan appeared to differ from previously suggested lifestyles for close relatives identified in hot springs in Yellowstone National Park, USA. The present study identified various microenvironmental gradients and niche differentiation enabling the co-existence of diverse chlorophototrophs in metabolically diverse communities in hot springs.

Key words: photosynthetic bacteria, hot springs, microbial diversity, vertical distribution, 16S rRNA gene amplicon sequences

Microbial mats are stratified assemblages of microbes and exopolymers that may develop into thick perennial microbial communities in extreme aquatic environments such as hot springs and hypersaline waters. These communities have a limited microbial diversity due to the extreme environmental conditions, and hot spring microbial mats constitute natural model systems for studying microbial diversity, ecophysiology, and population dynamics (6, 40, 51).

In light-exposed hot springs, microbial mats are dominated by phototrophic bacteria at temperatures between 42–74°C (70), and the microbial community composition and distribution of these mats exhibit niche differentiation along steep vertical gradients of light, water temperatures, and O₂ concentrations (26, 39, 45, 46). Previous studies have mostly focused on the importance of phototrophic organisms for primary production in the mats (10, 35, 57), and phototrophic bacteria have been shown to play important biogeochemical roles in facilitating oxygen production, sulfide consumption, and carbon fixation, among others (19, 21, 30, 36, 54, 56). Numerous chemotrophic organisms (*e.g.*, sulfate reducers, nitrogen fixers, and H₂ producers and consumers) co-exist and interact with phototrophs in nutrient cycling within microbial mats (7, 43, 48, 54, 62, 63, 65).

Microbial community compositions in phototrophic hot spring microbial mats have been studied worldwide, including Russia (9, 19, 55), Chile (34), China (30), and the USA (25, 62, 64, 68). Well-developed phototrophic mats characterized by a green upper layer and orange undermat have been studied extensively in the alkaline Octopus Spring and Mushroom Spring in Yellowstone National Park (YNP, USA) (25, 62, 63). Similar mat characteristics have been observed in Nakabusa hot springs in Japan, which have been actively studied for the last few decades (7, 14, 24, 39, 40, 42–44, 46, 48, 59). Mushroom Spring and Nakabusa hot springs are both slightly alkaline (pH 8.0 and ~8.5, respectively) hot springs with similar water chemistries (20, 52). In both hot springs, phototrophic microbial mats with similar characteristics (*e.g.*, a green upper layer over an orange-colored undermat) and communities develop (15, 22). Green mats developing at approx. 60°C in both springs contain oxygenic cyanobacteria, anoxygenic phototrophic *Chloroflexi*, as well as sulfate-reducing, sulfur-oxidizing, and fermenting chemotrophic bacteria (7, 25, 48). Although the community is highly similar at the phylum and class levels and sometimes at the genus level, it generally differs in the inhabiting species.

Microbial mats developing in the slightly alkaline Nakabusa hot springs form various green, brown, orange, and red-colored mats depending on the temperature and biogeochemical conditions in the effluent channels of the springs (15, 39).

* Corresponding author. E-mail: vthiel@tmu.ac.jp;
Tel: +81-42-677-2582; Fax +81-42-677-2559.

Previous studies reported the presence of various phototrophic as well as non-phototrophic members in these hot spring mats. The discovery of *Chloroflexus (Cfl.) aggregans* and *Roseiflexus (Rof.) castenholzii* (13, 14) demonstrated the occurrence of filamentous anoxygenic phototrophic bacteria in green mats developing at 40–65°C, typically in close association with oxygenic cyanobacteria (46). Nakagawa and Fukui (39) initiated a molecular study on microbial community structures in different-colored mats and streamers developing at temperatures of 48–76°C in Nakabusa hot springs and detected markedly different communities below and above 60°C. Microbial mats at lower temperatures were predominated by phototrophic bacteria, while mats at or above 66°C consisted of purely chemotrophic members. Another study on this hot spring found that cyanobacteria were the main component at 52°C up to approximately 60°C (7), while anoxygenic phototrophic bacteria, but not cyanobacteria, were detected in olive-green microbial mats at 65°C in addition to purely chemoautotrophic microbial streamers containing sulfate-reducing members at 75°C (27). Successive increases in the diversity of oxygenic and anoxygenic phototrophic bacteria were found to occur with decreasing temperatures in Nakabusa hot springs (7). In the present study, we selected microbial mats that developed in a small pool in Nakabusa hot springs with temperatures between 56 and 64°C, which contained both oxygenic and anoxygenic phototrophic bacteria, to study the vertical distribution of phototrophs in these mat communities.

The effects of environmental factors, such as temperature and light quality (different wavelengths), on the composition of microbial mat communities have already been investigated in Nakabusa hot spring microbial mats (20, 42, 59); however, the mechanisms by which the vertical distribution of microbial community members changes over seasons as affected by the vertical gradients of light and oxygen at this hot spring remain unknown. To clarify how the vertical distribution of phototrophs and the most abundant chemotrophic microbial community correlate with the microenvironmental gradients of light and oxygen, we examined green microbial mats

developing in a small pool in Nakabusa hot springs. In the present study, we used a combination of microsensors to assess environmental parameters (*i.e.*, light quality and oxygen concentrations) and 16S rRNA gene amplicon sequence analyses to identify microbial community members and elucidate their vertical distribution in hot spring phototrophic mats. We also described the diversity and stability of phototrophic microbial mat communities.

Materials and Methods

Sample collections and sites

Nakabusa hot springs (Nagano Prefecture, Japan) contain two characteristic sampling sites, the ‘Wall Site=Site A’ and ‘Stream Site=Site B’, as described by Nishihara and colleagues (43). In the present study, samples of microbial mats were taken from a small pool of a slightly alkaline hot spring (\approx pH 8.9) at ‘Stream Site=Site B’ at six different time points (36°23’33”N, 137°44’52”E; Fig. 1, Table S1) and were characterized by a green upper layer and orange undermat. Water temperature in the pool over the years has varied between 56 and 64°C. In November 2016, two sets of triplicate mat samples were taken, sequenced separately, and averaged, while single samples were taken and analyzed at all other time points. Microbial mat samples (thickness of approx. 3 mm) were taken in June, July, and November 2016 using a #4 cork borer (diameter of 7 mm, used for a bulk community analysis) and another set of mat samples (thickness of approx. 5 mm, separated into individual layers and used in an analysis of vertical distribution) were taken in May and November 2017 using a 4-cm modified cork borer made out of a falcon tube (Table S1). Samples for the bulk community analysis were cut at a depth of 3 mm, while samples taken in May and November 2017 were separated into five different (thickness of approx. 1 mm) layers with a sterile scalpel, and each layer was placed in a separate 2-ml screw cap collection tube. Samples were immediately frozen on dry ice on-site and kept at –80°C in the laboratory for further processing.

Microsensor measurements of light and oxygen

Measurements of O₂ over depth were conducted *in situ* in the microbial mat and overlying spring water in November 2016 at approximately 10:00 AM (Fig. 2) using electrochemical O₂ microsensors as previously described (18). In order to match the sampling time of the layered samples in November 2017, microsensor data

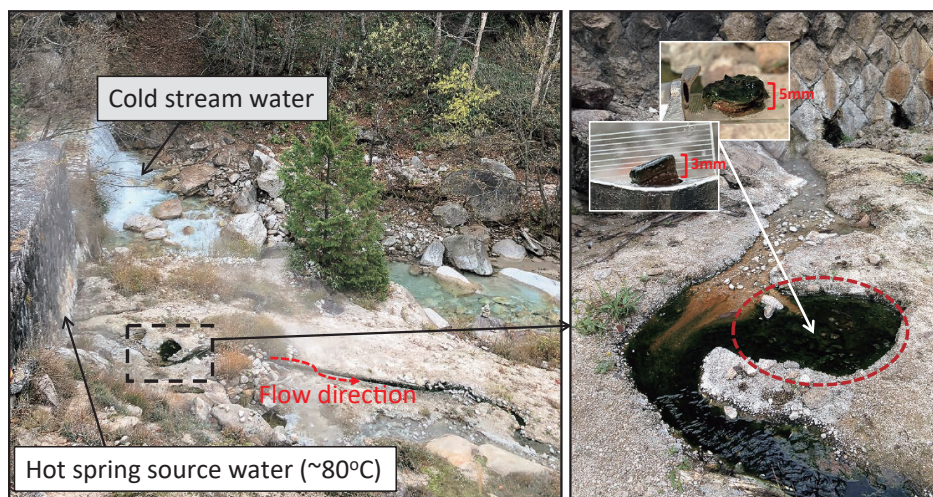


Fig. 1. Nakabusa hot springs (Nagano Pref., Japan) “Stream Site=Site B” showing a small pool with green microbial mats (dashed square in the left photo) and enlarged in the right photo. The sampled area is circled in red. Temperatures at the sampling area ranged between 56 and 64°C depending on the sampling time points (Table S1). The inset in the right photo shows representative samples of the mat taken from the sampling point.

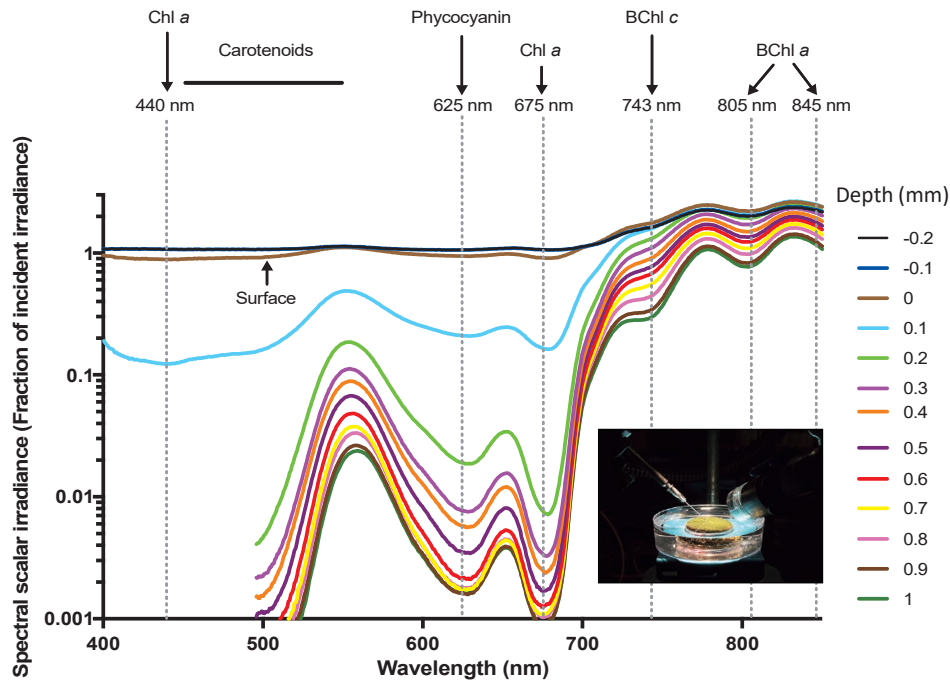


Fig. 2. Spectral scalar irradiance measured in different depths in the hot spring microbial mat (inset photo) in November 2016 (Sample GP_56). Absorption maxima of photopigments corresponding to minima/shoulders in the scalar irradiance spectra are indicated with arrows and dashed vertical lines.

from the same time of day in November 2016 are presented here (10:00 AM) (Fig. 2). O_2 concentrations were measured using a Clark-type O_2 sensor (OX25; Unisense A/S, Aarhus, Denmark) with a tip diameter of $<25 \mu\text{m}$, low stirring sensitivity ($<1\text{--}2\%$), and fast response time ($T_{90} < 0.5 \text{ s}$). Microsensors were mounted in a custom-made sensor holder, mounted on a motorized micromanipulator (Unisense A/S), and connected to a PC-interfaced microsensor multimeter (Unisense A/S), both were controlled by dedicated data acquisition and positioning software (SensorTrace Pro; Unisense A/S). Microsensors were carefully positioned at the mat surface (defined as $0 \mu\text{m}$) by manual operation of the micromanipulator.

Intact microbial mat samples were brought back to the laboratory for analyses of spectral light penetration using fiber-optic scalar irradiance microsensors (29, 53) according to Nielsen *et al.* (41). The depth profiles of photon scalar irradiance in the mat were measured with fiber-optic scalar irradiance microprobes with a sphere diameter of $80 \mu\text{m}$ and an isotropic angular response (53). The scalar irradiance microprobe was connected to a fiber-optic spectrometer (USB2000+; Ocean Optics, Florida, USA) interfaced to a PC running spectral acquisition software (Spectra Suite; Ocean Optics). Light was provided vertically from above by a fiber optic tungsten halogen lamp (KL2500-LCD; SCHOTT Benelux B.V., Culemborg, Netherlands) equipped with a collimating lens, while the scalar irradiance microprobe was inserted into the mat at a 45° angle. All measurements were performed in a dark room to avoid stray light. Profiles of photon scalar irradiance were measured in vertical steps of 0.1 mm from 0.2 mm above the surface until no more light was detectable. Incident light was quantified as downwelling photon scalar irradiance from the fiber optic tungsten halogen lamp with the fiber optic microprobe positioned over a black, non-reflective light well at a distance and position in the light field that was similar to the position of the mat surface; in a collimated light field, downwelling irradiance and downwelling scalar irradiance are identical (28). Absolute incident photon irradiance (PAR, $400\text{--}700 \text{ nm}$; in $\mu\text{mol photons m}^{-2} \text{ s}^{-1}$) was measured with a calibrated photon irradiance meter (ULM-500; Heinz Walz GmbH, Effeltrich, Germany) equipped with a spherical sensor (US-SQS/L; Heinz Walz GmbH) positioned in the light well at a distance similar to the position of the mat surface. The acquired spectra (corrected for dark noise) were integrated over the spectral

regions of interest, *i.e.*, PAR ($400\text{--}700 \text{ nm}$), and the integral was related to the absolute incident photon irradiance to obtain the amount of photosynthetic active radiation at each measuring depth expressed as fractions of incident photon scalar irradiance.

DNA extraction and sequencing

Genomic DNA was isolated from different bulk mat samples as well as separated layers of mats taken from the sampling site. Samples in June and July of 2016 were extracted based on a chloroform-phenol extraction method in combination with the cetyl trimethylammonium bromide (CTAB) method previously described by Nishihara *et al.* (43) (Table S1). Samples from November 2016, May 2017, and November 2017 were processed using the MO BIO PowerBiofilm DNA extraction kit (Qiagen, Hilden, Germany) following the manufacturer's protocol. Briefly, microbial mat samples ($0.11\text{--}0.21 \text{ g}$) were centrifuged prior to extraction to remove excess liquid. All centrifugation procedures were performed at $13,000\times g$ at room temperature. Homogenization was performed using FastPrep-24 (MP Biomedicals, Irvine, CA, USA) for 1 cycle at 5 m s^{-1} for 30 s . DNA was eluted in $100 \mu\text{L}$ BF7 solution, purified, and quantified following the protocol of the dsDNA Broadrange (BR) assay (Life Technologies, Grand Island, NY, USA) using a Qubit 3.0 fluorometer (Invitrogen, Carlsbad, CA, USA). Purified DNA (15 ng) was used to amplify the V4 region of 16S rRNA genes using 515F and 806R primers (4). PCR products in duplicate were pooled, purified, and quantified following the dsDNA BR assay using the Qubit 3.0 fluorometer. Purified PCR products (15 ng) were subjected to paired-end sequencing ($2\times 250 \text{ nt}$) using the Illumina Miseq platform (Illumina, San Diego, CA, USA) at FASMAC (Atsugi, Japan).

Sequence analysis

Sequence analyses were performed as described previously by Nishihara *et al.* (43) with the difference of the clustered Operational Taxonomic Units (OTUs) of the samples taken in 2016, which were originally classified using the Greengenes 13-8 reference database (37), being reclassified together with the 2017 samples using the SILVA database (Silva_128 release in February 2017). Briefly, raw data obtained from Illumina sequencing were quality filtered and analyzed using Quantitative Insights Into Microbial Ecology (QIIME)

(ver 1.9.0) (3). The remaining sequences were clustered into OTUs at a $\geq 97\%$ nucleotide sequence identity level and classified as described above. OTUs were identified using BLAST (Basic Local Alignment Search Tool) in NCBI (<https://blast.ncbi.nlm.nih.gov/>) as well as by phylogenetic analyses using the ARB software package (33). Phylogenetic trees based on 16S rRNA gene sequences were reconstructed using the Maximum Likelihood method with the GTR Model in the ARB software package (33). The robustness of tree topologies was tested with 100 bootstrap replicates.

Thirty-seven OTUs were selected in the present study based on the mean abundance of $\geq 0.5\%$ in two sets of triplicated microbial mat samples taken from one of the sampling time points (Nov 2016). The relative abundance of each OTU at the different time points was computed based on the total number of reads after the removal of singletons at each time point (Table S2) (67). The mean abundance and standard deviation (SD) of all OTUs based on the six time points were calculated. Additionally, low abundance OTUs ($< 0.2\%$) with the predicted phototrophic lifestyle were included in the analysis. Each of the OTUs was then compared based on their mean abundance and occurrence in all or only some of the six different time points. Core community members were identified as OTUs that occur in all samples and have a minimum relative abundance of $> 0.003\%$ in each of the sampling time-points. Species richness estimation (Chao1) was assessed using the online program SpadeR (Species-richness Prediction and Diversity Estimation in R) (5). The diversity and evenness of the taxa from six sampling time points were assessed based on the Shannon Index of Diversity (H'). Vertical distribution data were processed based on relative abundance as described above. The *t*-test was employed to compare the significance of differences between the mean relative sequence abundance of the vertical distribution of phototrophs and the most abundant chemotrophs between May 2017 and November 2017.

Nucleotide sequence accession numbers

The nucleotide sequences reported in the present study were deposited in the DDJB/EMBL/NCBI GenBank database with the following accession numbers LC461540–LC461576.

Results

Light penetration and O_2 distribution in the microbial mat

The spectral composition of scalar irradiance markedly changed over the first millimeter (mm) within the mat (Fig. 2). Light attenuation peaks were assigned to the characteristic absorption spectra of the photosynthetic pigments of phototrophs as previously described (8, 46). Wavelengths corresponding to the absorption maxima of photosynthetic pigments, such as Chl *a* (440 and 675 nm), carotenoids (450–550 nm), and phycocyanin (~620 nm), were strongly absorbed in the upper zone and showed increased attenuation from a depth of 0.2 to 0.9 mm. A shoulder in the scalar irradiance spectra also indicated the presence of low amounts of Chl *f* in the upper 0.3 mm of the mat (~710–720 nm) (46). Collectively, these spectral signatures indicated the presence of dense populations of oxygenic phototrophs in the upper layer of the mat. Near infrared radiation (NIR) was less strongly attenuated in this mat layer, and ~20–80% of incident irradiance remained at a depth of 1 mm. The NIR part of the scalar irradiance spectra showed distinct spectral minima corresponding to the absorption maxima of BChl *c* (~743 nm) and BChl *a* (~805 and 845 nm), which became stronger with increases in depths, indicating the increasing abundance of anoxygenic phototrophic bacteria below the uppermost 1 mm of the microbial mat.

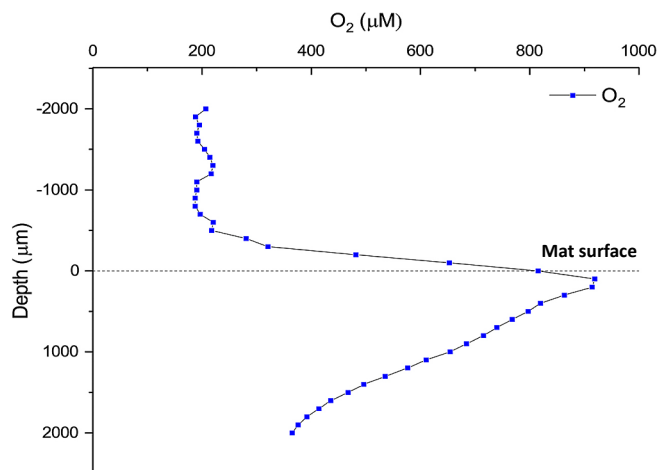


Fig. 3. *In situ* microsensor measurements of O_2 concentrations versus depth in the mat in the Nov. 2016 sampling. The time (10:00 AM) shown in this figure was selected based on the sampling time in November 2017 when mats were sampled for the vertical distribution study.

Oxygen concentrations were measured *in situ* in the upper 2 mm of the mat at a selected measurement time (at 10:00 AM; Fig. 3) during sampling in November 2016. The O_2 concentration in the overlaying water was ~200 μM , but increased in the diffusive boundary layer above the mat surface and reached a peak concentration of 900 μM 0.2–0.3 mm below the mat surface before steadily decreasing towards deeper mat layers.

Diversity of phototrophic and most abundant chemotrophic members of the community

The diversity and relative abundance of microbial populations in the phototrophic mats were assessed based on the OTUs of 16S rRNA gene amplicon sequences. High species richness estimates (Chao1, Table 1) were obtained due to the high number of singleton sequences (Table S2), which are generally undetected or rare species that are mostly concentrated on low frequencies (5). Variations in Chao1 estimates between the different time points negatively correlated with the total read numbers, *i.e.*, the sequencing depth. The three time points with high total read numbers (GP_56, GPL_56_M, and GPL_56_N; Table S2), which were averaged from multiple cores and layers, respectively, showed less singleton sequences and lower Chao1 estimates. The lower Chao1 estimates were assumed to be closer to the ‘real’ species richness in the mats. The number of OTUs for each sampling time-point ranged between 452 and 947 with abundance between 2 to 33,510 reads per OTU. Diversity was assessed by the Shannon Diversity Index having a mean value of 4.12 (Table 1), which was similar to previous diversity evaluations (4.71) of the microbial community in Nakabusa hot springs (42). The community was characterized by low evenness (Fig. S1) and was dominated by only a few OTUs in the present study (Table 2), similar to microbial mat communities from Mushroom Spring in YNP (USA) (63).

Among the thirty-seven OTUs (Fig. 4), twenty-five core community members (highlighted in Table 2) that frequently occurred in all samples were identified in the phototrophic mat at a temperature range of 56–64°C. Nine out of the twenty-

Table 1. Diversity indices based on sequence reads of OTUs from six sampling time points.

Sample Code	Date of Sampling	Chao1	CV (%)	OTUs*	H'	H_{max}	E
GP_61	2016 June	24130	90.5	947	4.58	6.85	0.67
GP_64	2016 July	23161	90.6	868	4.86	6.77	0.72
GP_57	2016 July	20482	91.7	866	4.37	6.76	0.65
GP_56	2016 Nov	5952	98.8	708	3.69	6.56	0.56
GPL_56_M	2017 May	4421	99.1	859	4.02	6.76	0.60
GPL_56_N	2017 Nov	5613	98.8	452	3.22	6.11	0.53
Mean		13960	94.9	783	4.12	6.64	0.62
SD		9544	4.4	180	0.60	0.27	0.07

Chao1—Species richness estimation with singleton and doubleton sequences calculated by SpadeR (5)

CV—Coverage estimate of the entire dataset

OTUs*—number of OTUs without singleton

H' —Shannon Diversity Index

H_{max} (maximum diversity of a sample) = $\ln S$ (normal logarithm of S), where S is the total number of OTUs

E—Evenness = H'/H_{max}

five OTUs were highly abundant ($\geq 1\%$ mean relative abundance): four were phototrophic bacteria, three were anoxygenic phototrophic bacteria, and one was an oxygenic cyanobacterium. The most abundant OTU, NK_OTU-002 (19.5% mean relative abundance) represents the anoxygenic phototrophic *Chloroflexi* (Fig. S2) member *Rof. castenholzii* with 100% nucleotide sequence identity to the type strain HL08^T previously isolated from the Nakabusa mats (14). The second most abundant member, *Cfl. aggregans* NK_OTU-001 (17.6% mean relative abundance) belonging to the same phylum (Fig. S2), was also previously detected in these mats (NKB_63_10) (7) and is 99% identical to *Cfl. aggregans* type strain MD-66^T (NCBI Acc. NR_074226) (13). The third most abundant anoxygenic phototrophic filamentous *Chloroflexi* that was frequently detected in all samples, NK_OTU-006, represents a close relative to “*Candidatus* (*Ca.*) *Roseilinea gracile*” (62), which was initially detected in Mushroom Spring in YNP in a metagenomic analysis (63, 64) and is currently being examined for isolation and characterization (62). The same organism was found to increase in sequence abundance when subjected to an *in situ* light experiment in Nakabusa hot springs (42), supporting its phototrophic lifestyle. Another abundant phototroph, NK_OTU-003 is 100% identical to *Thermosynechococcus* sp. NK55 (58), which is a known oxygenic phototroph in these mats belonging to *Cyanobacteria* (Fig. S3).

The five other highly abundant core community members, NK_OTU-007, 028, 012, 023, and 051, are predicted to be chemotrophic members of the community, representing three bacterial phyla (Table 2). They are uncultured species and only have 85–96% similarities to the nearest type strains. Among this group, NK_OTU-007 represents the phylum *Acidobacteria* (Fig. S4) and is the most abundant chemotrophic member in this community (5.9% mean relative abundance). It is identical to OTU ‘denovo3451’ (100% nucleotide sequence similarity) previously detected in Nakabusa hot springs (43) and 96% identical to the *Acidobacteria* clone YNP_SBC_BP4_B26 from YNP (38). The phylum *Armatimonadetes* (Fig. S5) is represented by NK_OTU-028 in the present study, which is also higher in abundance than other chemotrophs (4.3% mean relative abundance). This member is 100% identical to an uncultured clone sequence obtained from Nakabusa at 56°C (7) and closely related to clone MS-B_OTU-03 from Mushroom Spring (63) and uncultured *Eubacterium* sp. OS-L from Octopus Spring (69) with 98 and 96% nucleotide

sequence similarities, respectively. The results of a partial genome analysis indicated aerobic or microaerobic metabolism for the YNP mat member (63).

Three abundant core community members representing the super phylum *Chlorobi/Bacteroidetes/Ignavibacteria* (Fig. S6) were detected in these mats (OTUs NK_OTU-12, -23, and -51, Table 2). NK_OTU-012 belongs to ‘*Chlorobi* lineage 2’ (Fig. S6) and has 100% sequence identity with the NKB_56_U2 clone previously recovered from Nakabusa hot springs (7) and is 99% identical to *Chlorobi* clone SM1H02, which was initially detected in the Mammoth hot spring, YNP (NCBI Acc. AF445702). NK_OTU-023 represents an uncultured member of ‘*Chlorobi* lineage 5’ (also known as “clade OPB56” and/or “*Ca.* *Kapabacteria*”, Fig. S6), which is 100% identical to the clone MS-B_OTU-24 detected from Mushroom Spring in 2012 (63). Another ‘*Chlorobi* lineage 5’ member, NK_OTU-51 (Fig. S6), which is 99% similar to the clone MS-B_OTU-29 recovered from Mushroom Spring, YNP, is predicted to represent the newly discovered putative sulfate-reducing bacterium “*Ca.* *Thermonerobacter thiotrophicus*” (63, 66).

Other core members of the microbial community in Nakabusa hot springs are frequently occurring in all samples, but are less abundant (ranging between 0.2 and 0.9% mean relative abundance). Among the sixteen OTUs detected, only one member, the *Alphaproteobacteria* member NK_OTU-032 (Fig. S7), was related to a strain with predicted phototrophic ability, while all others were putative chemotrophic species (Table 2). NK_OTU-032 is 98% identical to “*Ca.* *Roseovibrio tepidum*” strain MS-P3, which was initially detected in Mushroom Spring (YNP) in 2015 and is a novel BChl-*a* containing α -proteobacterial species (62). This strain shows 16S rRNA gene sequence similarities to the *Roseomonas* and *Rhodovarius* spp. strains. However, in contrast to non-phototrophic *Roseomonas* species, such as *R. estuarii*, this is the only member of this group that produces BChl *a* and contains *pufLM* genes (encoding for the L and M subunits of the type-2 photosynthetic reaction center) (63), suggesting a chlorophototrophic lifestyle.

Twelve OTUs representing six phyla were only detected at a relative abundance of $<0.003\%$ at some time points (Table 2). Five of these OTUs were classified as phototrophs based on their closest relative belonging to four phyla. The phylum *Chloroflexi* (Fig. S2) is represented by two filamentous ano-

Table 2. Taxonomic affiliation and mean relative abundance of 37 selected microbial community members from six sampling time points based on 16S rRNA amplicon sequence reads. OTU selection was based on one of the sampling time points (November 2016) with $\geq 0.5\%$ relative sequence abundance. Identities were based on nucleotide sequence similarities with their closest relatives in NCBI databases using BLAST hits.

Phylum	OTU-name	Mean Relative Abundance	Min	Max	SD	Relevant BLAST Hits	Acc. No.	Identity (% nt)	
<i>Chloroflexi</i>	NK_OTU-002 ^P	19.5%	5.21%	38.20%	12.31%	clone NLEA-OTU2 (Nakabusa hot springs, Japan) <i>Roseiflexus castenholzii</i> HLO8 ^T	MF435938 NR_112114	100 100	
	NK_OTU-001 ^P	17.6%	2.64%	31.09%	9.34%	clone NKB_63_10 (Nakabusa hot springs, Japan) <i>Chloroflexus aggregans</i> DSM 9485 ^T	JF826984 NR_074226	100 99	
	NK_OTU-006 ^P	1.8%	1.04%	2.94%	0.92%	clone NLEA-OTU120 (Nakabusa hot springs, Japan) “ <i>Candidatus</i> Roseilinea gracile” (Mushroom Spring, YNP, USA) <i>Leptolinea tardivitalis</i> YMTK-2 ^T	MF435983 KY937207 NR_040971	100 96 88	
	NK_OTU-014	0.3%	0.10%	0.88%	0.30%	clone NLEA-OTU35 (Nakabusa hot springs, Japan) clone iTag MS-B_2012_OTU-9 (Mushroom Spring, YNP, USA) <i>Thermomarinilinea lacunifontana</i> SW7 ^T	MF435955 KU860149 NR_132293	100 99 92	
	NK_OTU-222 ^P	0.5%	0.0%	2.85%	1.16%	clone NLEA-OTU27 (Nakabusa hot springs, Japan) “ <i>Candidatus</i> Chloranaerofilum corporosum” (Mushroom Spring, YNP, USA) <i>Oscillochloris trichoides</i> DG-6 ^T	MF435959 KY937209 AF146832	100 98 92	
	NK_OTU-092 ^P	0.2%	0.0%	1.08%	0.43%	<i>Chloroflexus</i> sp. clone Alla12-1 (Alla hot spring, Russia) <i>Chloroflexus aurantiacus</i> J-10-fl ^T	KP701483 NR_074263	100 100	
	<i>Cyanobacteria</i>	NK_OTU-003 ^P	6.5%	3.35%	10.74%	2.69%	<i>Thermosynechococcus</i> sp. NK55 (Nakabusa hot springs, Japan) <i>Thermosynechococcus elongatus</i> PKUAC-SCTE731	CP006735 MF405428	100 100
NK_OTU-007		5.9%	0.18%	13.71%	5.69%	uncultured denovo34541 (Nakabusa hot springs, Japan) <i>Acidobacteria</i> clone YNP_SBC_BP4_B26 (Lower Geyser Basin, YNP, USA) <i>Chloracidobacterium thermophilum</i> D	LC381388 HM448257 KP300942	100 96 87	
<i>Acidobacteria</i>	NK_OTU-046	0.6%	0.25%	1.47%	0.47%	clone NLEA-OTU13 (Nakabusa hot springs, Japan) <i>Acidobacteria</i> clone Tyva_DA_OTU_0059 (Hydrothermal spring, Russia) <i>Paludibaculum fermentans</i> P105 ^T	MF435947 MG950134 NR_134120	100 100 95	
	NK_OTU-15047 ^P	0.001%	0.0%	0.01%	0.003%	clone iTag MS-B_2012_OTU-17 (Mushroom Spring, YNP, USA) <i>Chloracidobacterium thermophilum</i> D	KU860157 KP300942	100 97	
<i>Armatimonadetes</i>	NK_OTU-028	4.3%	0.08%	14.28%	5.84%	clone NKB_56_N2 (Nakabusa hot springs, Japan) clone iTag MS-B_2012_OTU-3 (Mushroom Spring, YNP, USA) <i>Eubacterium</i> sp. (OS type L) (Octopus Spring, YNP, USA)	JF826973 KU860143 L04707	100 98 96	
	NK_OTU-012	1.7%	0.07%	4.89%	1.67%	clone NKB_56_U2 (Nakabusa hot springs, Japan) <i>Chlorobi</i> clone SM1H02 (Mammoth hot springs, YNP, USA) <i>Ignavibacterium album</i> JCM16511 ^T	JF826976 AF445702 NR_074698	100 99 89	
	NK_OTU-023	1.7%	0.59%	5.77%	2.05%	clone iTag MS-B_2012_OTU-24 (Mushroom Spring, YNP, USA) Uncultured <i>Rhodothermus</i> sp. clone 9 (Porcelana hot spring, Chile) “ <i>Candidatus</i> Rhodothermus clarus”	KU860164 MH938161 AB252420	100 99 85	
<i>Chlorobi/ Bacteroidetes/ Ignavibacteria</i>	NK_OTU-051	1.0%	0.08%	3.35%	1.08%	<i>Chlorobi</i> clone: HGM-D-87 (Geothermal water, Kagoshima, Japan) clone iTag MS-B_2012_OTU-29 (Mushroom Spring, YNP, USA) <i>Ignavibacterium album</i> JCM16511 ^T	AB539665 KU860169 NR_074698	99 99 81	
	NK_OTU-008	0.8%	0.01%	2.04%	0.81%	<i>Bacteroidetes</i> clone Tyva_DA_OTU_0019 (Hydrothermal spring, Russia) <i>Ignavibacterium album</i> JCM16511 ^T	MG950110 NR_074698	100 95	
	NK_OTU-259	1.0%	0.0%	5.77%	2.35%	clone NLEA-OTU41 (Nakabusa hot springs, Japan) clone SJA-28 (Germany) <i>Thauera mechernichensis</i> TL1 ^T	MF435972 AJ009458 NR_026473	100 88 87	
	NK_OTU-021 ^P	0.1%	0.0%	0.62%	0.25%	<i>Chlorobium</i> sp. clone 4 (Porcelana hot spring, Chile) clone OS-GSB (Octopus Spring, YNP, USA) <i>Chloroherpeton thalassium</i> ATCC 35110 ^T	MH938157 KU565869 NR_074270	99 91 92	
	NK_OTU-005	2.9%	0.0%	14.09%	5.62%	<i>Bacteroidetes</i> clone A5-00YK9 (Boekleung hot spring, Thailand) Candidate division OP clone M2UF07 (YNP, USA) <i>Lewinella maritima</i> HME9321 ^T	EU376411 FJ885732 NR_158053	99 95 89	
	NK_OTU-004	1.2%	0.0%	4.90%	2.01%	clone NLEA-OTU36 (Nakabusa hot springs, Japan) clone iTag MS-B_2012_OTU-196 (Mushroom Spring, YNP, USA) <i>Pedobacter steynii</i> DSM19110 ^T	MF435960 KU860334 MH929833	99 92 84	
	NK_OTU-016	0.2%	0.0%	0.84%	0.33%	<i>Bacteroidetes</i> clone YNP_SBC_MS3_B92 (Lower Geyser Basin, YNP, USA) clone Tat-08-003_12_90 (El Tatio Geyser Field, Chile) <i>Solitalea longa</i> HR-AV ^T	HM448200 GU437354 MF685247	97 96 89	
	<i>Aquificae</i>	NK_OTU-010	0.9%	0.19%	2.33%	0.80%	uncultured denovo14971 (Nakabusa hot springs, Japan) <i>Sulfurihydrogenibium azorense</i> Az-Fu1 ^T <i>Sulfurihydrogenibium yellowstonense</i> SS-5 ^T	LC381396 NR_102858 NR_043111	100 100 94
		NK_OTU-019	0.4%	0.08%	0.76%	0.28%	uncultured denovo29919 (Nakabusa hot springs, Japan) clone dongzy2tff41747 (Tibet hot spring, China) <i>Thermocrinis jamiesonii</i> GBS1 ^T	LC381395 KU482385 NR_145905	100 97 96
		NK_OTU-015	0.4%	0.06%	0.88%	0.32%	<i>Hydrogenobacter</i> sp. clone Tsenher12otu8-10 (Tsenher hot spring, Mongolia)	KT258797	100
uncultured denovo15700 (Nakabusa hot springs, Japan) <i>Hydrogenobacter subterraneus</i> HGPI ^T							LC381391 NR_024729	100 99	

Table 2. Continued.

Phylum	OTU-name	Mean Relative Abundance	Min	Max	SD	Relevant BLAST Hits	Acc. No.	Identity (% nt)
Planctomycetes	NK_OTU-009	0.9%	0.17%	2.10%	0.83%	Uncultured <i>Eubacterium</i> env. OPS 3 (Obsidian Pool, YNP, USA)	AF018188	100
						“ <i>Candidatus</i> Gemmata massiliana” IIL29	NR_148576	95
	NK_OTU-033	0.4%	0.12%	1.10%	0.38%	clone TP19 (Tibet hot spring, China)	EF205574	99
						clone iTag MS-B_2012_OTU-51 (Mushroom Spring, YNP, USA) <i>Thermogutta terrifontis</i> R1 ^T	KU860191 NR_134826	98 90
Thermodesulfobacteria	NK_OTU-013	0.3%	0.003%	0.97%	0.44%	uncultured denovo155 (Nakabusa hot springs, Japan)	LC381408	100
						<i>Caldimicrobium thiodismutans</i> TF1 ^T	NR_148865	100
						<i>Caldimicrobium rimae</i> DS ^T	NR_044283	97
Proteobacteria	NK_OTU-030	0.4%	0.10%	0.69%	0.22%	clone Alla1 lotu10-1 (Alla hot spring, Russia)	KP676764	99
						clone NLEA-OTU15 (Nakabusa hot springs, Japan)	MF435964	99
						<i>Thermomonas hydrothermalis</i> SGM-6 ^T	NR_025265	92
	NK_OTU-032 ^P	0.6%	0.43%	0.99%	0.22%	clone B35 (Great Artesian Basin, Australia)	AF407720	100
						clone NLEA-OTU29 (Nakabusa hot springs, Japan)	MF435979	99
						“ <i>Candidatus</i> Roseovibrio tepidum” MS-P3	MG821467	98
Deinococcus-Thermus	NK_OTU-031	1.2%	0.0%	3.61%	1.64%	clone iTag MS-B_2012_OTU-92 (Mushroom Spring, YNP, USA)	KU860232	100
						clone QL15B_6pJ (Queen’s Laundry hot spring, YNP, USA)	KU382142	100
						“ <i>Candidatus</i> Desulfacinum subterraneum”	AF385080	90
	NK_OTU-017	0.1%	0.0%	0.81%	0.33%	<i>Desulfomicrobium</i> sp. 21	KX018622	100
						<i>Desulfomicrobium thermophilum</i> DSM 16697 ^T	MH741285	99
Firmicutes	NK_OTU-279 ^P	0.02%	0.0%	0.11%	0.04%	<i>Elioraea</i> sp. clone 5 (Porcelana hot spring, Chile)	MH938158	100
						<i>Elioraea tepidiphila</i> TU-7 ^T	NR_044259	100
						“ <i>Candidatus</i> Elioraea thermophila” MS-B_OTU-4	MH555907	94
	NK_OTU-025	0.5%	0.10%	0.94%	0.27%	clone NKB_56_02 (Nakabusa hot Springs, Japan)	JF826974	100
					<i>Meiothermus luteus</i> YIM 72257 ^T	NR_157749	99	
Spirochaetae	NK_OTU-018	0.4%	0.11%	0.79%	0.24%	uncultured denovo15330 (Nakabusa hot Springs, Japan)	LC381401	100
						<i>Firmicutes</i> clone YNP_SBC_BP3_B7	HM448232	95
						<i>Thermodesulfitimonas autotrophica</i> SF97 ^T	NR_156074	87
Nitrospirae	NK_OTU-011	0.3%	0.07%	1.18%	0.43%	clone iTag MS-B_2012_OTU-25 (Mushroom Spring, YNP, USA)	KU860165	100
						clone NKB48 (Nakabusa hot springs, Japan)	FR691784	100
						<i>Leptonema illini</i> 3055 ^T	NR_043139	86
Parcubacteria	NK_OTU-020	0.9%	0.08%	2.19%	0.78%	clone NLEA-OTU9 (Nakabusa hot springs, Japan)	MF435944	100
						clone NKB_63_50 (Nakabusa hot springs, Japan)	JF826987	100
						<i>Thermodesulfobivrio yellowstonii</i> DSM 11347 ^T	NR_074345	94
	NK_OTU-514	0.2%	0.0%	1.11%	0.45%	clone G19 (Great Artesian Basin, Australia)	AF407702	100
						“ <i>Candidatus</i> Nitrospira calida” (Geothermal spring, Austria)	HM485589	96
Parcubacteria	NK_OTU-034	0.2%	0.05%	0.46%	0.17%	clone HGM-U-39 (Geothermal water, Kagoshima, Japan)	AB539626	96
						clone iTag MS-B_2012_OTU-222 (Mushroom Spring, YNP, USA)	KU860360	88
						<i>Parcubacteria</i> group bacterium GW2011_GWC1_41_7	KX123526	79

highlighted—Core members of the community (OTU was detected in all samples and with relative abundance of $\geq 0.003\%$ in each of the sampling time points)

^P—phototrophic member based on its closest relative

^T—type strain

nt—nucleotide sequence similarity

0.0%—relative abundance reads of $<0.003\%$ or zero sequence reads

ygenic chlorophototrophs, *Chloroflexus* sp. NK_OTU-092, which corresponds to *Cf. aurantiacus* J-10-fl^T (NCBI Acc. NR_074263) (49), and NK_OTU-222 with 98% sequence similarity to the *Oscillochloris*-like chlorophototroph “*Ca. Chloranaerofilum corporosum*”, a novel BChl *c* containing filamentous anoxygenic phototrophic member of *Chloroflexi* initially detected in Mushroom Spring, YNP (62). The latter was exclusively detected in the undermat of Mushroom Spring and expected to prefer the anaerobic environment of the deeper layers of the mat (63). NK_OTU-021 may represent an unusual phototrophic member of the phylum *Chlorobi*, “*Ca. Thermochlorobacter aerophilum*”, the first aerobic, photoheterotrophic *Chlorobi* that was initially detected in Octopus Spring, YNP (32, 62). An anoxygenic phototrophic proteobacterium, represented by NK_OTU-279 in the present study represents a member of the genus *Elioraea* (Fig. S7),

with 100 and 94% nucleotide sequence similarities to *Elioraea tepidiphila* TU-7^T (1) and “*Ca. Elioraea thermophila*”, respectively (Table 2). Although the type strain has been described as a chemotroph, members of this genus are hypothesized to be aerobic anoxygenic phototrophs based on the presence of photosynthesis-related genes in their genomes as well as their ability to synthesize BChl *a* under aerobic conditions (62). Similar to the low-abundance member found in the mat community at 60°C in Mushroom Spring (63), *Elioraea* sp. NK_OTU-279 was also found to be low in abundance in Nakabusa hot springs in the present study. Another low-abundance, less frequently occurring OTU, NK_OTU-15047, putatively represents a novel species of the phototrophic *Acidobacteria* genus *Chloracidobacterium* (*Cab.*) (97% nucleotide sequence similarity to *Cab. thermophilum* strain B^T) (2, 11, 60, 61).

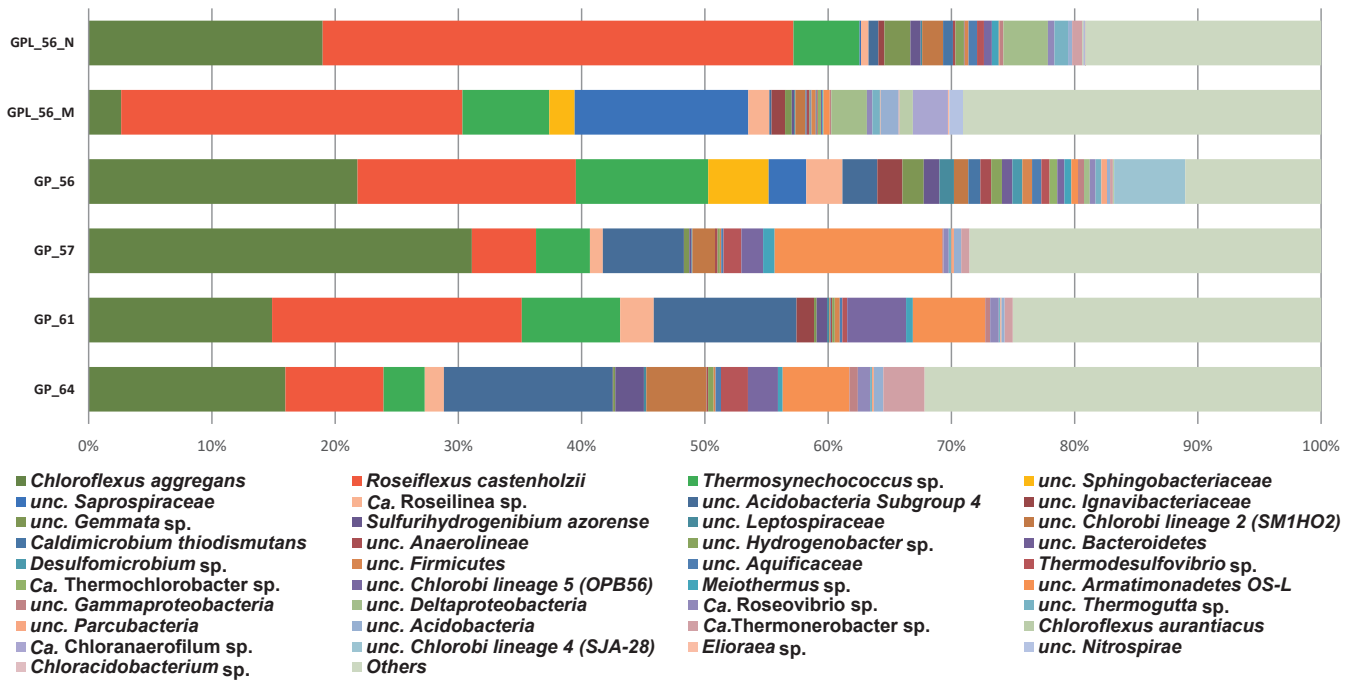


Fig. 4. Microbial community based on 16S rRNA gene amplicon sequences at the species level. Thirty-seven selected OTUs, which all showed $\geq 0.5\%$ mean relative abundance in the two sets of triplicate samples in November 2016, were included for this figure. The identities of the OTUs were based on the SILVA database (Silva_128 released in February 2017) and NCBI database (2018). Sample codes on the left side indicate different sampling time points and temperatures during sampling (GPL_56_N-Nov 2017, 56°C; GPL_56_M-May 2017, 56°C; GP_56-Nov 2016, 56°C; GP_57-July 2016, 57°C; GP_61-June 2016, 61°C; GP_64-July 2016, 64°C).

We only found few sequences (<100 sequence reads) that were related to *Leptolyngbia* sp. Nb3F1 (Fig. S3) in the present study. *Leptolyngbia*-like NK_OTU-090 was only 91% similar to the Chl-*f* producing *Leptolyngbia* spp. detected in a previous study (46); however, this may indicate another species of Chl-*f* producing cyanobacteria in the microbial mats at Nakabusa hot springs.

Vertical distribution of phototrophic community members

At two of the time points (May 2017 and November 2017), the mat was separated into five layers that were individually analyzed by 16S rRNA gene amplicon sequencing, disclosing the vertical distribution of different phototrophic and chemotrophic mat members. The sequences of the phototrophic members varied with depth, as shown in Fig. 5. Sequences representing the oxygenic phototroph *Thermosynechococcus* sp., (NK_OTU-003) were similarly abundant ($P>0.05$, Table S3) at both time points and showed a clear decrease in relative abundance with depth (Fig. 5). Sequences representing this cyanobacterium were mainly found in layers 1 and 2, representing the first 2 mm of the mat and correlating with the green color of the upper mat layer as well as strong absorbance at 675 nm (indicating the presence of Chl *a*) in the first 1 mm (Fig. 2). Relative abundance in the second layer was higher in the May sample, correlating with longer and stronger sunlight periods in summer.

Among the anoxygenic phototrophs, sequences representing the most abundant member of the phylum *Chloroflexi*, BChl *a*-containing *Rof. castenholzii* (NK_OTU-002) did not significantly differ ($P>0.05$, Table S3) between the two sampling periods (May and November 2017). Sequences markedly

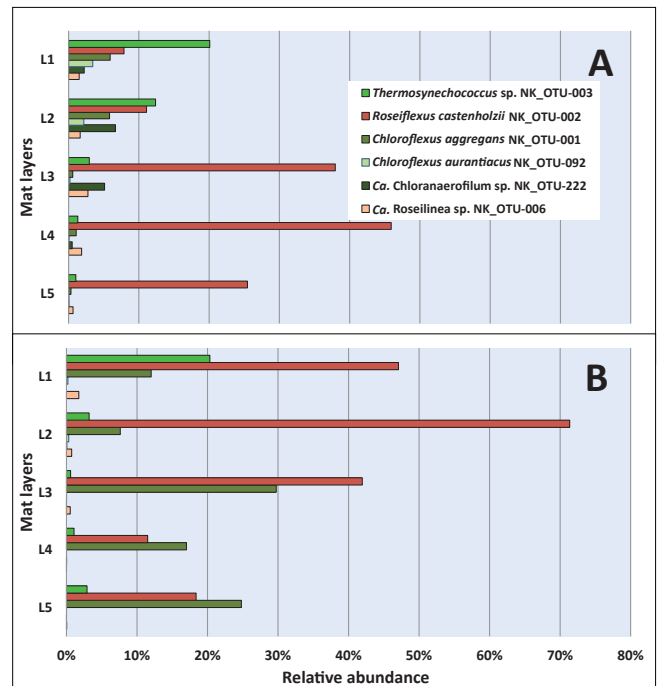


Fig. 5. Vertical distribution of phototrophic members of *Chloroflexi* and *Cyanobacteria* based on 16S rRNA gene amplicon sequences in May 2017 (A) and November 2017 (B). Mat layers are indicated by L1 to L5 (L1- uppermost layer; L5- bottom layer).

varied among layers (Fig. 5), with the highest relative abundance of *Rof. castenholzii* being observed in layer 4 in May 2017 (Fig. 5A) and layer 2 in the winter sample (November

2017) (Fig. 5B). The higher abundance of BChl *a*-containing *Rof. castenholzii* sequences in deeper layers correlated with the relatively higher light penetration of NIR into deeper layers, particularly in the summer (Fig. 2 and 5A). Differences in the layer with the highest relative sequence abundance for this organism between the two sampling times correlated with the different light conditions between the two seasons. The higher competitiveness of *Rof. castenholzii* in the lower layers may be explained by the avoidance of competition with other phototrophic bacteria, *e.g.*, cyanobacteria and other FAPs; or the active avoidance of high light conditions in the upper layers. The abundance of sequences representing the oxygen-tolerant filamentous anoxygenic phototroph, *Cfl. aggregans* (NK_OTU-001), significantly differed ($P < 0.05$, Table S3) between the two seasons, with higher abundance in winter (Nov 2017, 18.35% mean relative abundance) than in summer (May 2017, 2.75% mean relative abundance). Within the mats, *Cfl. aggregans* sequences clearly showed decreasing relative abundance with depth in May 2017 (Fig. 5A), with relatively high abundance in the first two upper layers of the mat. In contrast, in November 2017 (Fig. 5B), overall abundance was markedly higher, indicating the stronger competitiveness of this member in the winter than in the summer months. This correlates with the presence of BChl *c*-containing light-harvesting organelles, the chlorosomes, in this organism, which are often found in low-light-adapted phototrophs such as green sulfur bacteria (47). Another phototrophic member, “*Ca. Roseilinea sp.*” NK_OTU-006 also showed significant differences ($P = 0.05$, Table S3) in average abundance between the two sampling seasons, with higher relative abundance in May than in November 2017. This member does not contain BChl *c* or chlorosomes and relies entirely on BChl *a* for its phototrophic growth (62), and, thus, is not as low-light adapted as *Chloroflexus* spp. Furthermore, the vertical distribution of “*Ca. Roseilinea sp.*” NK_OTU-006 differed between the two samplings. The relative abundance of sequences was the highest in layer 3 in May 2017 (Fig. 5A), and in the uppermost layer in November 2017 (Fig. 5B), indicating that irradiance supporting this phototroph penetrated less deeply into the mats in winter. Alternatively, oxygen concentrations were hypothesized to be less favorable (*e.g.*, too high) in the upper layers in May or too low in November in the deeper layers because this organism has been suggested to be an oxygen-tolerant or -dependent anoxygenic phototroph, possibly with the need for microoxic conditions, as has been shown for another phototrophic mat member, *Cab. thermophilum* (61). The two less abundant members of the phylum *Chloroflexi*, *Cfl. aurantiacus* (NK_OTU-092) and “*Ca. Chloranaerofilum sp.*” (NK_OTU-222), showed no significant differences ($P > 0.05$, Table S3) between seasons (May 2017 and Nov 2017). However, the sequence abundance of these members among the five layers varied with depth. Anoxygenic filamentous phototrophic *Cfl. aurantiacus* sequences were relatively high in the upper two layers for both seasons, indicating requirements for light and/or oxygen. On the other hand, sequences representing “*Ca. Chloranaerofilum sp.*” (NK_OTU-222), showed the highest relative abundance in the second layer for both sampling seasons, suggesting a preference for lower light and/or oxygen concentrations than *Cfl. aurantiacus* (Fig. 2 and 3). However, in contrast to previous studies on “*Ca.*

Chloranaerofilum corporosum” in hot spring mats in YNP, the member of this microbial mat community in Nakabusa did not appear to prefer completely anoxic conditions, as suggested previously (62).

The vertical distributions of less abundant phototrophic members represented by three phyla (*Chlorobi*, *Acidobacteria*, and *Proteobacteria*) (Fig. S4, S6, and S7) were also analyzed based on the relative abundance of sequences in the five layers (Fig. 6). “*Ca. Thermochlorobacter sp.*” NK_OTU-021 (*Chlorobi*) was only detected in May 2017 (Fig. 6A), with the highest relative abundance (0.67%) being observed in the uppermost layer and markedly decreasing with depth, correlating with the suggested need and tolerance for high oxygen concentrations for its next relative “*Ca. Thermochlorobacter aerophilum*” (32). Another less abundant member in these mats, *Chloracidobacterium sp.* NK_OTU-15047, was only detected in November 2017 (Fig. 6B) with unexpectedly varying abundance (ranging between 0.01 and 0.02%) from the upper to the lower layer despite its known microaerophilic lifestyle (61). Two less abundant phototrophic members in these mats represent the phylum *Proteobacteria*, “*Ca. Roseovibrio sp.*” NK_OTU-032 and *Elioraea sp.* NK_OTU-279. “*Ca. Roseovibrio sp.*” NK_OTU-032 showed no significant differences ($P > 0.05$, Table S3) in the average relative abundances of sequences for the two sampling periods. In a comparison of the relative abundance in five layers, this member showed higher abundance in the second layer representing 1.23 and 0.91% of mean relative sequence abundance in May 2017 and November 2017 (Fig. 6), respectively. A decrease in the relative abundance of sequences was detected after the second layer for both seasons, suggesting the preference of (micro)aerobic or (low-)light conditions. The other proteobacterial member,

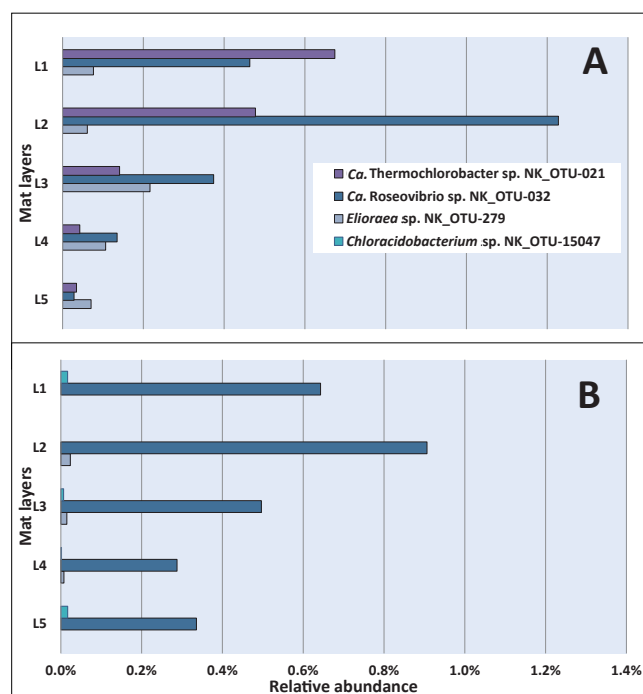


Fig. 6. Vertical distribution of less abundant phototrophic members of *Proteobacteria*, *Chlorobi*, and *Acidobacteria* based on 16S rRNA gene amplicon sequences in May 2017 (A) and November 2017 (B). Mat layers are indicated by L1 to L5 (L1-uppermost layer; L5-bottom layer).

Elioraea sp. NK_OTU-279, representing a putative aerobic anoxygenic phototroph, showed significant differences ($P < 0.05$, Table S3) in the averaged relative abundance of sequences between sampling seasons with higher abundance in May 2017 than in November 2017 (Fig. 6). Despite this difference, the vertical distribution of this OTU demonstrated that the organism showed the highest relative abundance in the middle layer in both sampling seasons (layer 3), which correlated with its assumed microaerophilic physiology (62).

Vertical distribution of the most abundant chemotrophic community members

The distribution of abundant chemotrophic community members was also analyzed based on the relative abundance of sequences among the five separated layers of these mats (Fig. 7). As shown in Table 2, five out of the nine most abundant members of these community members corresponded to uncultured, putatively chemotrophic species (NK_OTU-007, 012, 023, 028, and 051). Three members, NK_OTU-012, OTU-023, and OTU-051, representing the phylum *Chlorobi* (Fig. S6), were all related to sequences previously detected in hot spring environments in YNP and predicted to have chemoheterotrophic lifestyles (16, 17, 23, 63, 66). The relative abundance of sequences did not significantly differ ($P > 0.05$, Table S4) between May 2017 and November 2017, suggesting that these core members were relatively stable in abundance over time. The vertical distribution of the uncultured ‘*Chlorobi* lineage 2’ (SM1H02) represented by NK_OTU-012 and NK_OTU-51 related to “*Ca. Thermonerobacter thiotrophicus*” (66) in the ‘OPB56 clade’ (*Chlorobi* lineage 5, “*Ca. Kapabacteria*”) showed that the relative abundance of these

sequences increased with depth, reflecting higher abundance in the anaerobic zones of the mats (Fig. 3 and 7) and indicating a putatively anaerobic lifestyle. Another ‘*Chlorobi* lineage 5’ (OPB56 clade, “*Ca. Kapabacteria*”) member, NK_OTU-023, showed the highest relative sequence abundance in the second and third layers in May 2017 (0.17% mean relative abundance) and November 2017 (1.2% mean relative abundance), respectively, which indicates a preference for microaerobic environments (Fig. 7).

Other abundant putatively chemotrophic members representing two phyla (*Acidobacteria* and *Armatimonadetes*) (Fig. S4 and S5) also did not significantly differ ($P > 0.05$, Table S4) in relative sequence abundance for the two sampling seasons. However, the vertical distribution of *Acidobacteria* member NK_OTU-007 showed the highest relative abundance of sequences in the uppermost layer of the mats, in which cyanobacteria were present and high oxygen concentrations occurred during the day (Fig. 3) and decreased with depth (Fig. 7), indicating a possible aerobic metabolism in both seasons. In contrast to previous studies, sequences representing the uncultured OS-L like *Armatimonadetes* member NK_OTU-028 showed high relative abundance in the lower layers, specifically in the fourth and fifth layers in May and November 2017, respectively (Fig. 7), indicating putatively anaerobic metabolism.

Discussion

The diversity, relative abundance, and depth-dependent distribution of the hot spring-associated phototrophic microbial community at Nakabusa hot springs “Stream site=Site B” were revealed in the present study based on 16S rRNA gene amplicon sequencing. This method is suitable for identifying different community members and estimating their relative abundance through sequence reads, but does not disclose their metabolic activity or physiological capacity or ability. The mean diversity index obtained in the present study was similar to that reported previously in Nakabusa hot springs (42) and did not markedly change among the six sampling time points, indicating a stable microbial mat community, which is uneven and dominated by only a few community members (Table 1 and Fig. S1). The core community consists of nine abundant and sixteen less abundant members present in all the samples analyzed (Table 2). The characteristic layering of the green top layer and orange-colored undermat observed in the mats in the present study were also found in phototrophic microbial mats in many hot springs worldwide (9, 22, 34, 50, 55, 63, 64, 72). The green upper layer correlated with the presence of oxygenic cyanobacteria in the upper 1 to 2 mm of the mat, with their photosynthetic pigments giving the layer its characteristic color, while the orange-colored undermat only contained anoxygenic phototrophic and chemotrophic members (Fig. 5–7).

Microbial mats from Nakabusa hot springs were dominated by phototrophic species (Fig. 4 and Table 2), with additional chemotrophic organisms co-existing. Overall, ten different phototrophic bacteria were detected in these mats. Consistent with previous findings, the oxygenic cyanobacteria, *Thermosynechococcus* sp. (58) and filamentous anoxygenic phototrophs (FAPs), *Cfl. aggregans* (13) and *Rof. castenholzii*

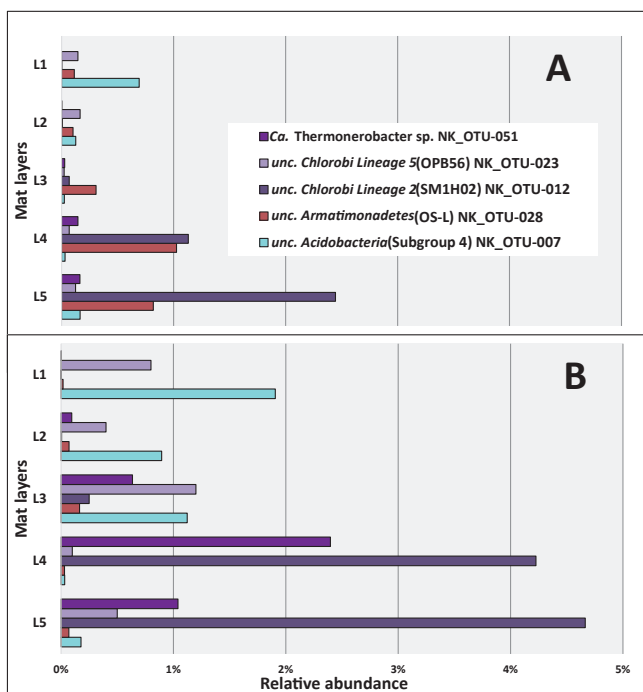


Fig. 7. Vertical distribution of the most abundant ($\geq 1\%$) chemotrophic members of *Chlorobi*, *Armatimonadetes*, and *Acidobacteria* based on 16S rRNA gene amplicon sequences in May 2017 (A) and November 2017 (B). Mat layers are indicated by L1 to L5 (L1-uppermost layer; L5-bottom layer).

(14) were identified as the most abundant phototrophic members in the Nakabusa mats in this study (7, 27, 39, 48). Less abundant previously described phototrophs, such as *Cfl. aurantiacus* (12) and *Chloracidobacterium* sp., were also detected. Additionally, some unusual and novel phototrophic members from three phyla (*Elioraea* sp. and “*Ca. Roseovibrio* sp.”, *Proteobacteria*; “*Ca. Thermochlorobacter* sp.”, *Chlorobi*; “*Ca. Roseilinea* sp.” and “*Ca. Chloranaerofilum* sp.”, *Chloroflexi*) were identified in Nakabusa hot springs for the first time, while closely related species have been detected in Mushroom Spring, suggesting their more universal distribution in hot spring environments (62, 65). The presence of some of these phototrophs in Nakabusa hot springs was previously reported by cultivation and microscopy studies (e.g., *Chloracidobacterium* sp. and “*Ca. Thermochlorobacter* sp.”; Y. Shirotori and M. Tank, unpublished data). This illustrates the importance of the combination of traditional and modern techniques in the discovery and identification of unusual, novel, and low-abundance members in these hot spring mats.

Nine members from five bacterial phyla and dominated by the phylum *Chloroflexi* (Fig. S2), including four phototrophs were consistently found in high abundance in these mats (Fig. 4). Similar to the undermat community in Mushroom Spring mats in YNP, *Roseiflexus* spp. was identified as the most abundant member (63), while in contrast to the YNP study, *Cfl. aggregans* co-existed as the second most abundant member in Nakabusa (Table 2). Both FAPs have been detected in these mats before and their phototrophic metabolism in the mats has been supported by *in situ* experiments (42). In addition to ribosomal gene sequences, the presence of these FAPs was demonstrated in the present study by their characteristic photosynthetic pigments BChl *a* and *c* based on the absorption peaks at 743 and 845 nm in the first upper millimeter (Fig. 2). The different photosynthetic pigments allow the two phototrophic *Chloroflexi* members to inhabit different ecological niches and depths in these mats (Fig. 5, and 6). Differences in abundance and depth distribution for these FAPs in the mats between the summer and winter samples may be due to the different light intensities in these seasons. For example, during the high-light season (summer), NIR light penetrates deeper into the mats, allowing the dominating red FAP *Rof. castenholzii* to grow phototrophically in the lower layers of the mat, while they were found closer to the surface in the low-light season (winter) (Fig. 5). In addition to light, oxygen also plays an important role as the determining factor for the vertical distribution of these FAPs (and other mat community members) (Fig. 3). Both species are known to grow phototrophically in the absence of oxygen only, while both have been shown to be additionally able to grow chemotrophically under aerobic dark conditions (13–15). The lower abundance of oxygenic phototrophic cyanobacteria in the mats in winter may be assumed to lead to lower oxygen concentrations, particularly in the intermediate and deeper layers of the mat, thereby facilitating the anoxygenic phototrophic growth of the FAPs. In addition, the light-harvesting apparatus, the so-called chlorosomes, allow *Cfl. aggregans* to efficiently grow under low-light conditions, possibly leading to the higher relative abundance observed in these mats in winter (Fig. 5). Thus, a combination of several factors, including oxygen and light, is hypothesized to shape

the environmental conditions leading to the niche separation, vertical distribution, and competitiveness of the different mat members (Fig. 2 and 3). The closely related species *Cfl. aurantiacus*, which is inconsistently present and at markedly lower numbers in Nakabusa spring mats, shows very similar metabolism and growth physiology to *Cfl. aggregans*. Its presence in the upper layers of the mat in the summer sample (Fig. 5A) confirms the described oxygen tolerance for this species and facultative aerobic chemoheterotrophic metabolism (49).

“*Ca. Roseilinea gracile*”, an unusual and novel *Anaerolineae*-like *Chloroflexi* member and predicted red FAP containing BChl *a* was initially detected in YNP (31, 62–64). A recent genomic study placed this organism in the proposed new class “*Ca. Thermofonsia*”, a sister class of *Anaerolineae* from which it may be distinguished particularly by their predicted aerobic metabolism (71) (Fig. S2). Although not as abundant as *Rof. castenholzii*, sequences representing “*Ca. Roseilinea* sp.” showed a similar vertical distribution, *i.e.*, presence in deeper layers in summer than in winter, which may be attributed to the predicted deeper penetration of NIR light into the mats in summer (Fig. 5). The next relative of the least abundant chlorophototrophic *Chloroflexi*, “*Ca. Chloranaerofilum* sp.” has been suggested to synthesize BChls *a* and *c* to capture light (64). In contrast to the reported strict anaerobic lifestyle of “*Ca. Chloranaerofilum corporosum*” in Mushroom Spring, YNP (62), the high relative abundance in the second layer of “*Ca. Chloranaerofilum* sp.” in the summer sample (Fig. 5A) indicates tolerance to oxygen (Fig. 3). With only 98% nucleotide sequence identity compared to the proposed type species “*Ca. Chloranaerofilum corporosum*” (62), this phototroph recovered from Nakabusa hot springs appears to represent a new species of “*Ca. Chloranaerofilum*”, with different metabolic traits, such as oxygen requirements or tolerance.

An additional four phototrophic bacteria were detected at a lower abundance and/or inconsistently (“*Ca. Roseovibrio* sp.” NK_OTU-032, *Elioraea* sp. NK_OTU-279 (*Proteobacteria*), “*Ca. Thermochlorobacter* sp.” (*Chlorobi*), and *Chloracidobacterium* sp. (*Acidobacteria*)) in the mats (Fig. S4, S5, and S6). The next relatives of the two phototrophic *Proteobacteria* in these mats, “*Ca. Roseovibrio* sp.” NK_OTU-032 and *Elioraea* sp. NK_OTU-279, have been suggested to have similar growth patterns with respect to photosynthetic pigment compositions and tolerance to oxygen; both species contain BChl *a* and grow under aerobic conditions (62). Differences in the vertical distribution of the two members, as shown in Fig. 6, indicate slightly different ecological niches and potentially different preferences or needs for oxygen concentrations and/or light intensity. Nucleotide sequence identities of 98 and 94% between the sequences obtained in the present study and the proposed type strain species “*Ca. Roseovibrio tepidum*” strain MS-P3 (62) and “*Ca. Elioraea thermophila*” clone MS-B_OTU-4 (62), respectively, indicate different species and possibly even genera for the organisms in Nakabusa. The phototrophic *Chlorobi* member “*Ca. Thermochlorobacter* sp.” NK_OTU-021 represents a close relative to “*Ca. Thermochlorobacter aerophilum*”. The latter was initially detected in microbial mats from YNP using metagenomics as well as metatranscriptomic analyses (25, 32) and is the first aerobic photoheterotrophic member of

the phylum *Chlorobi*, a phylum that is known for its strictly anaerobic sulfur-oxidizing chlorophototrophic members, the green sulfur bacteria (32). Despite being less frequently detected in the samples, the vertical distribution of “*Ca. Thermochlorobacter* sp.” NK_OTU-021 sequences in May 2017 revealed that the sequences of this chlorophototroph were the most abundant in the uppermost portion of the mat (Fig. 6A), in which the oxygenic phototrophic cyanobacteria, *Thermosynechococcus* spp., were the most abundant, thereby supporting the suggested need for high oxygen concentrations for this novel phototrophic member of *Chlorobi* (32, 62). Only a few sequences related to *Chloracidobacterium* sp. (NK_OTU-15047) were obtained in the present study. Based on the close similarity (97% nucleotide sequence identity) to the type strain *Cab. thermophilum*, a microaerophilic chlorophototrophic lifestyle may be assumed (60).

The vertical distribution of different chemotrophic members in the mats positively or negatively correlates with oxygen concentrations obtained in the present study (Fig. 3). For example, the abundant chemoheterotrophic “*Ca. Thermonerobacter* sp.” represented by NK_OTU-051 in the present study, increased in abundance with depth (Fig. 7), suggesting preferred growth in the anaerobic layers of the mats. It has recently been described as a putative anaerobe with dissimilatory sulfate-reducing metabolism by metagenomic and metatranscriptomic analyses (66). Therefore, its highest abundance in deeper, anaerobic layers in these mats is consistent with the general occurrence of sulfate reducers in anaerobic niches (7, 27, 39). In addition to the anaerobic respiration of sulfate, aerobic respiration in this bacterium was suggested from the findings of metagenomic analyses (66), which may be responsible for the detection of this organism in the microaerobic middle layer of the mat (Fig. 7). An increase in sequence abundance with depth indicating an anaerobic lifestyle was also observed for other abundant chemotrophic members of the mats, such as the uncultured ‘Chlorobi lineage 2’ (SM1HO2) member represented by NK_OTU-012 (Fig. 7). In contrast, uncultured ‘Chlorobi lineage 5’ NK_OTU-023 appears to tolerate oxygen in the middle to upper layers, suggesting a microaerobic or aerobic lifestyle. The uncultured *Armatimonadetes* member NK_OTU-028, similar to “Type OS-L” obtained from Mushroom and Octopus Springs in YNP, shows a vertical distribution indicating a possible microaerobic lifestyle, while previous studies suggested aerobic metabolism for the YNP mat member (Fig. 7) (59, 64). This indicates high metabolic versatility for different species, populations, or ecotypes, and correlates with predicted microdiversity in this taxonomic group, as suggested previously (63). Another abundant chemoheterotrophic member, the uncultured *Acidobacteria* member NK_OTU-007 was present in all samples, indicating a stable presence as a member of the core community in these mats. The vertical distribution of this mat member clearly revealed an indication for microaerobic to aerobic metabolism, which is further supported by the results of the metagenome analysis (Fig. 7, unpubl. data, Martinez *et al.*, in preparation).

Conclusion

Green phototrophic microbial mats developing at approx. 60°C in Nakabusa hot springs (Nagano, Japan) consisted of a low diversity core community of nine abundant ($\geq 1\%$ mean relative sequence abundance) members, as well as approximately 28 low-abundance and variable community members in this 16S rRNA gene amplicon sequencing study. Ten different phototrophic bacteria were identified, representing five out of seven known phyla containing phototrophic members; three anoxygenic phototrophic *Chloroflexi* and one oxygenic *Cyanobacteria* species dominated the community. Oxygenic cyanobacteria were limited to the green upper 2-mm depth of the mat, as identified by 16S rRNA gene sequences and irradiance absorption spectra. Anoxygenic phototrophs were additionally found in the lower orange-colored layers, which correlated with the penetration of NIR light deeper into the mat. The vertical distribution of the different phototrophic bacteria indicates a number of ecological niches in part driven by micro-environmental gradients with regard to light and oxygen. This niche differentiation enables the co-existence of diverse chlorophototrophs in metabolically diverse communities in these mats. Furthermore, five abundant ($\geq 1\%$) uncultured chemotrophic members with different lifestyles varying from predicted aerobic and microaerobic to anaerobic metabolism showed positive and negative correlations, respectively, with oxygen concentrations in their vertical distribution. Further studies on metabolic potential using metagenome sequence data (Martinez *et al.*, in preparation) will provide a better insight and further clarify the diversity and ecological potentials of the microbial mat community members in Nakabusa hot springs.

Acknowledgements

The authors would like to thank the Tokyo Human Resources Fund for City Diplomacy (JNM) and the Institute of Fermentation Osaka (IFO) for funding this research. This study was further supported by the ‘Encouraging Young Scientist Research Fund at the Tokyo Metropolitan University’ (VT) and grants from the Independent Research Fund Denmark | Natural Sciences (MK; DFF-8021-00308B and DFF-1323-00065B). We are grateful to Mr. Takahito Momose (the owner of Nakabusa hot springs) for allowing us to stay and collect samples from the hot springs. Thank you to Prof. Katsumi Matsuura for the joint collection of microbial mats and to Photosynthetic Microbial Consortia Lab members for all the help.

References

1. Albuquerque, L., F.A. Rainey, M.F. Nobre, and M.S. da Costa. 2008. *Elioraea tepidiphila* gen. nov., sp. nov., a slightly thermophilic member of the *Alphaproteobacteria*. *Int. J. Syst. Evol. Microbiol.* 58:773–778.
2. Bryant, D.A., A.M.G. Costas, J.A. Maresca, *et al.* 2007. *Candidatus Chloracidobacterium thermophilum*: An aerobic phototrophic *Acidobacterium*. *Science* 317:523–526.
3. Caporaso, J.G., J. Kuczynski, J. Stombaugh, *et al.* 2010. QIIME allows analysis of high-throughput community sequencing data. *Nat. Methods* 7:335–336.
4. Caporaso, J.G., C.L. Lauber, W.A. Walters, D. Berg-Lyons, C.A. Lozupone, P.J. Turnbaugh, N. Fierer, and R. Knight. 2011. Global patterns of 16S rRNA diversity at a depth of millions of sequences per sample. *Proc. Natl. Acad. Sci. U.S.A.* 108:4516–4522.

5. Chao, A., K.H. Ma, T.C. Hsieh, and C.-H. Chiu. 2015. Online Program SpadeR (Species-richness Prediction And Diversity Estimation in R). Program and User's Guide published at http://chao.stat.nthu.edu.tw/wordpress/software_download/.
6. de Beer, D., M. Weber, A. Chennu, T. Hamilton, C. Lott, J. Macalady, and J.M. Klatt. 2017. Oxygenic and anoxygenic photosynthesis in a microbial mat from an anoxic and sulfidic spring. *Environ. Microbiol.* 19:1251–1265.
7. Everroad, R.C., H. Otaki, K. Matsuura, and S. Haruta. 2012. Diversification of bacterial community composition along a temperature gradient at a thermal spring. *Microbes Environ.* 27:374–381.
8. Ferris, M.J., M. Kuhl, A. Wieland, and D.M. Ward. 2003. Cyanobacterial ecotypes in different optical microenvironments of a 68°C hot spring mat community revealed by 16S-23S rRNA internal transcribed spacer region variation. *Appl. Environ. Microbiol.* 69:2893–2898.
9. Gaisin, V.A., A.M. Kalashnikov, M.V. Sukhacheva, Z.B. Namsaraev, D.D. Barhutova, V.M. Gorlenko, and B.B. Kuznetsov. 2015. Filamentous anoxygenic phototrophic bacteria from cyanobacterial mats of Alla hot springs (Barguzin Valley, Russia). *Extremophiles* 19:1067–1076.
10. Gan, F., S. Zhang, N.C. Rockwell, S.S. Martin, J.C. Lagarias, and D.A. Bryant. 2014. Extensive remodeling of a cyanobacterial photosynthetic apparatus in far-red light. *Science* 345:1312–1317.
11. Garcia Costas, A.M., Z. Liu, L.P. Tomsho, S.C. Schuster, D.M. Ward, and D.A. Bryant. 2012. Complete genome of *Candidatus Chloracidobacterium thermophilum*, a chlorophyll-based photoheterotroph belonging to the phylum *Acidobacteria*. *Environ. Microbiol.* 14:177–190.
12. Hanada, S., A. Hiraishi, K. Shimada, and K. Matsuura. 1995. Isolation of *Chloroflexus aurantiacus* and related thermophilic phototrophic bacteria from Japanese hot springs using an improved isolation procedure. *J. Gen. Appl. Microbiol.* 41:119–130.
13. Hanada, S., A. Hiraishi, K. Shimada, and K. Matsuura. 1995. *Chloroflexus aggregans* sp. nov., a filamentous phototrophic bacterium which forms dense cell aggregates by active gliding movement. *Int. J. Syst. Bacteriol.* 45:676–681.
14. Hanada, S., S. Takaichi, K. Matsuura, and K. Nakamura. 2002. *Roseiflexus castenholzii* gen. nov., sp. nov., a thermophilic, filamentous, photosynthetic bacterium that lacks chlorosomes. *Int. J. Syst. Evol. Microbiol.* 52:187–193.
15. Hanada, S. 2003. Filamentous anoxygenic phototrophs in hot springs. *Microbes Environ.* 18:51–61.
16. Hiras, J., Y.-W. Wu, S.A. Eichorst, B.A. Simmons, and S.W. Singer. 2016. Refining the phylum *Chlorobi* by resolving the phylogeny and metabolic potential of the representative of a deeply branching, uncultivated lineage. *ISME J.* 10:833–845.
17. Iino, T., K. Mori, Y. Uchino, T. Nakagawa, S. Harayama, and K. Suzuki. 2010. *Ignavibacterium album* gen. nov., sp. nov., a moderately thermophilic anaerobic bacterium isolated from microbial mats at a terrestrial hot spring and proposal of *Ignavibacteria classis* nov., for a novel lineage at the periphery of green sulfur bacteria. *Int. J. Syst. Evol. Microbiol.* 60:1376–1382.
18. Jensen, S.I., A.-S. Steunou, D. Bhaya, M. Kuhl, and A.R. Grossman. 2011. *In situ* dynamics of O₂, pH and cyanobacterial transcripts associated with CCM, photosynthesis and detoxification of ROS. *ISME J.* 5:317–328.
19. Kalashnikov, A.M., V.A. Gaisin, M.V. Sukhacheva, B.B. Namsaraev, A.N. Panteleeva, E.N. Nuyanzina-Boldareva, B.B. Kuznetsov, and V.M. Gorlenko. 2014. Anoxygenic phototrophic bacteria from microbial communities of Goryachinsk thermal spring (Baikal Area, Russia). *Microbiology* 83:407–421.
20. Kato, K., T. Kobayashi, H. Yamamoto, T. Nakagawa, Y. Maki, and T. Hoaki. 2004. Microbial mat boundaries between chemolithotrophs and phototrophs in geothermal hot spring effluents. *Geomicrobiol. J.* 21:91–98.
21. Kawai, S., N. Kamiya, K. Matsuura, and S. Haruta. 2019. Symbiotic growth of a thermophilic sulfide-oxidizing photoautotroph and an elemental sulfur-disproportionating chemolithoautotroph and cooperative dissimilatory oxidation of sulfide to sulfate. *Front. Microbiol.* 10:1150.
22. Kim, Y.-M., S. Nowack, M.T. Olsen, *et al.* 2015. Diel metabolomics analysis of a hot spring chlorophototrophic microbial mat leads to new hypotheses of community member metabolisms. *Front. Microbiol.* 6:209.
23. Kim, Y.T., and E.D. Park. 2010. Water-gas shift reaction over supported Pt and Pt-CeOx catalysts. *Korean J. Chem. Eng.* 27:1123–1131.
24. Kimura, H., M. Sugihara, K. Kato, and S. Hanada. 2006. Selective phylogenetic analysis targeted at 16S rRNA genes of thermophiles and hyperthermophiles in deep-subsurface geothermal environments. *Appl. Environ. Microbiol.* 72:21–27.
25. Klatt, C.G., J.M. Wood, D.B. Rusch, *et al.* 2011. Community ecology of hot spring cyanobacterial mats: predominant populations and their functional potential. *ISME J.* 5:1262–1278.
26. Klatt, C.G., W.P. Inskeep, M.J. Herrgard, *et al.* 2013. Community structure and function of high-temperature chlorophototrophic microbial mats inhabiting diverse geothermal environments. *Front. Microbiol.* 4:106.
27. Kubo, K., K. Knittel, R. Amann, M. Fukui, and K. Matsuura. 2011. Sulfur-metabolizing bacterial populations in microbial mats of the Nakabusa hot spring, Japan. *Syst. Appl. Microbiol.* 34:293–302.
28. Kuhl, M., and B.B. Jorgensen. 1994. The light field of microbenthic communities: Radiance distribution and microscale optics of sandy coastal sediments. *Limnol. Oceanogr.* 39:1368–1398.
29. Kuhl, M. 2005. Optical microsensors for analysis of microbial communities, p. 166–199. *In* J.R. Leadbetter (ed.), *Methods in Enzymology*, vol. 397, Academic Press, New York.
30. Lau, M.C.Y., J.C. Aitchison, and S.B. Pointing. 2009. Bacterial community composition in thermophilic microbial mats from five hot springs in central Tibet. *Extremophiles* 13:139–149.
31. Liu, Z., C.G. Klatt, J.M. Wood, D.B. Rusch, M. Ludwig, N. Wittekindt, L.P. Tomsho, S.C. Schuster, D.M. Ward, and D.A. Bryant. 2011. Metatranscriptomic analyses of chlorophototrophs of a hot-spring microbial mat. *ISME J.* 5:1279–1290.
32. Liu, Z., C.G. Klatt, M. Ludwig, D.B. Rusch, S.I. Jensen, M. Kuhl, D.M. Ward, and D.A. Bryant. 2012. '*Candidatus* Thermochlorobacter aerophilum': an aerobic chlorophotoheterotrophic member of the phylum *Chlorobi* defined by metagenomics and metatranscriptomics. *ISME J.* 6:1869–1882.
33. Ludwig, W., O. Strunk, R. Westram, *et al.* 2004. ARB: a software environment for sequence data. *Nucleic Acids Res.* 32:1363–1371.
34. Mackenzie, R., C. Pedrós-Alió, and B. Diez. 2013. Bacterial composition of microbial mats in hot springs in Northern Patagonia: variations with seasons and temperature. *Extremophiles* 17:123–136.
35. Madigan, M.T. 2003. Anoxygenic phototrophic bacteria from extreme environments. *Photosynth. Res.* 76:157–171.
36. Madigan, M.T., D.O. Jung, E.A. Karr, W.M. Sattley, L.A. Achenbach, and M.T.J. van der Meer. 2005. Diversity of anoxygenic phototrophs in contrasting extreme environments, p. 203–220. *In* W.P. Inskeep, and T.R. McDermott (ed.), *Geothermal Biology and Geochemistry in Yellowstone National Park*, vol. 1. Montana State University Publications, Bozeman, MT.
37. McDonald, D., M.N. Price, J. Goodrich, E.P. Nawrocki, T.Z. DeSantis, A. Probst, G.L. Andersen, R. Knight, and P. Hugenholtz. 2012. An improved Greengenes taxonomy with explicit ranks for ecological and evolutionary analyses of bacteria and archaea. *ISME J.* 6:610–618.
38. Meyer-Dombard, D.R., W. Swingley, J. Raymond, J. Havig, E.L. Shock, and R.E. Summons. 2011. Hydrothermal ecotones and streamer biofilm communities in the Lower Geyser Basin, Yellowstone National Park. *Environ. Microbiol.* 13:2216–2231.
39. Nakagawa, T., and M. Fukui. 2002. Phylogenetic characterization of microbial mats and streamers from a Japanese alkaline hot spring with a thermal gradient. *J. Gen. Appl. Microbiol.* 48:211–222.
40. Nakagawa, T., and M. Fukui. 2003. Molecular characterization of community structures and sulfur metabolism within microbial streamers in Japanese hot springs. *Appl. Environ. Microbiol.* 69:7044–7057.
41. Nielsen, M., N.P. Revsbech, and M. Kuhl. 2015. Microsensor measurements of hydrogen gas dynamics in cyanobacterial microbial mats. *Front. Microbiol.* 6:726.
42. Nishida, A., V. Thiel, M. Nakagawa, S. Ayukawa, and M. Yamamura. 2018. Effect of light wavelength on hot spring microbial mat biodiversity. *PLoS One* 13:e0191650.
43. Nishihara, A., S. Haruta, S.E. McGlynn, V. Thiel, and K. Matsuura. 2018. Nitrogen fixation in thermophilic chemosynthetic microbial communities depending on hydrogen, sulfate, and carbon dioxide. *Microbes Environ.* 33:10–18.
44. Nishihara, A., V. Thiel, K. Matsuura, S.E. McGlynn, and S. Haruta. 2018. Phylogenetic diversity of nitrogenase reductase genes and possible nitrogen-fixing bacteria in thermophilic chemosynthetic microbial communities in nakabusa hot springs. *Microbes Environ.* 33:357–365.

45. Nowicka, B., and J. Kruk. 2016. Powered by light: Phototrophy and photosynthesis in prokaryotes and its evolution. *Microbiol. Res.* 186–187:99–118.
46. Ohkubo, S., and H. Miyashita. 2017. A niche for cyanobacteria producing chlorophyll *f* within a microbial mat. *ISME J.* 11:2368–2378.
47. Oostergetel, G.T., H. van Amerongen, and E.J. Boekema. 2010. The chlorosome: a prototype for efficient light harvesting in photosynthesis. *Photosynth. Res.* 104:245–255.
48. Otaki, H., R.C. Everroad, K. Matsuura, and S. Haruta. 2012. Production and consumption of hydrogen in hot spring microbial mats dominated by a filamentous anoxygenic photosynthetic bacterium. *Microbes Environ.* 27:293–299.
49. Pierson, B.K., and R.W. Castenholz. 1974. A phototrophic gliding filamentous bacterium of hot springs, *Chloroflexus aurantiacus*, gen. and sp. nov. *Arch. Microbiol.* 100:5–24.
50. Portillo, M.C., V. Sririr, W. Kanoksilapatham, and J.M. Gonzalez. 2009. Differential microbial communities in hot spring mats from Western Thailand. *Extremophiles* 13:321–331.
51. Ramsing, N.B., M.J. Ferris, and D.M. Ward. 2000. Highly ordered vertical structure of *Synechococcus* populations within the one-millimeter-thick photic zone of a hot spring cyanobacterial mat. *Appl. Environ. Microbiol.* 66:1038–1049.
52. Revsbech, N.P., E. Trampe, M. Lichtenberg, D.M. Ward, and M. Kühl. 2016. *In situ* hydrogen dynamics in a hot spring microbial mat during a diel cycle. *Appl. Environ. Microbiol.* 82:4209–4217.
53. Rickelt, L.F., M. Lichtenberg, E.C.L. Trampe, and M. Kühl. 2016. Fiber-optic probes for small-scale measurements of scalar irradiance. *Photochem. Photobiol.* 92:331–342.
54. Roeselers, G., T.B. Norris, R.W. Castenholz, S. Rysgaard, R.N. Glud, M. Kühl, and G. Muyzer. 2007. Diversity of phototrophic bacteria in microbial mats from Arctic hot springs (Greenland). *Environ. Microbiol.* 9:26–38.
55. Rozanov, A.S., A.V. Bryanskaya, T.V. Ivanisenko, T.K. Malup, and S.E. Peltek. 2017. Biodiversity of the microbial mat of the Garga hot spring. *BMC Evol. Biol.* 17:254.
56. Saer, R.G., and R.E. Blankenship. 2017. Light harvesting in phototrophic bacteria: structure and function. *Biochem. J.* 474:2107–2131.
57. Stal, L.J., H. Bolhuis, and M.S. Cretoiu. 2017. Phototrophic microbial mats. p. 295–318. *In* P.C. Hallenbeck (ed.), *Modern Topics in the Phototrophic Prokaryotes*. Springer, Cham.
58. Stolyar, S., Z. Liu, V. Thiel, *et al.* 2014. Genome sequence of the thermophilic cyanobacterium *Thermosynechococcus* sp. strain NK55a. *Genome Announc.* 2:e01060-13.
59. Sugiura, M., M. Takano, K. Shin-ichi, K. Toda, and S. Hanada. 2001. Application of a portable spectrophotometer to microbial mat studies: Temperature dependence of the distribution of cyanobacteria and photosynthetic bacteria in hot spring water. *Microbes Environ.* 16:255–261.
60. Tank, M., and D.A. Bryant. 2015. Nutrient requirements and growth physiology of the photoheterotrophic *Acidobacterium*, *Chloracidobacterium thermophilum*. *Front. Microbiol.* 6:1–14.
61. Tank, M., and D.A. Bryant. 2015. *Chloracidobacterium thermophilum* gen. nov., sp. nov.: an anoxygenic microaerophilic chlorophotoheterotrophic acidobacterium. *Int. J. Syst. Evol. Microbiol.* 65:1426–1430.
62. Tank, M., V. Thiel, D.M. Ward, and D.A. Bryant. 2017. A Panoply of Phototrophs: An overview of the thermophilic chlorophototrophs of the microbial mats of alkaline siliceous hot springs in Yellowstone National Park, WY, USA, p. 87–137. *In* P.C. Hallenbeck, *Modern Topics in the Phototrophic Prokaryotes*, Springer, Cham.
63. Thiel, V., J.M. Wood, M.T. Olsen, M. Tank, C.G. Klatt, D.M. Ward, and D.A. Bryant. 2016. The dark side of the Mushroom Spring microbial mat: Life in the shadow of chlorophototrophs. I. Microbial diversity based on 16S rRNA gene amplicons and metagenomic sequencing. *Front. Microbiol.* 7:919.
64. Thiel, V., M. Hügler, D.M. Ward, and D.A. Bryant. 2017. The dark side of the Mushroom Spring microbial mat: Life in the shadow of chlorophototrophs. II. Metabolic functions of abundant community members predicted from metagenomic analyses. *Front. Microbiol.* 8:943.
65. Thiel, V., M. Tank, and D.A. Bryant. 2018. Diversity of chlorophototrophic bacteria revealed in the omics era. *Annu. Rev. Plant Biol.* 69:21–49.
66. Thiel, V., A.M. Garcia Costas, N.W. Fortney, J.N. Martinez, M. Tank, E.E. Roden, E.S. Boyd, D.M. Ward, S. Hanada, and D.A. Bryant. 2019. “*Candidatus* Thermonerobacter thiotrophicus,” A non-phototrophic member of the *Bacteroidetes/Chlorobi* with dissimilatory sulfur metabolism in hot spring mat communities. *Front. Microbiol.* 9:3159.
67. Unno, T. 2015. Bioinformatic suggestions on MiSeq-based microbial community analysis. *J. Microbiol. Biotechnol.* 25:765–770.
68. Ward, D., and F. Cohan. 2006. Microbial diversity in hot spring cyanobacterial mats: Pattern and prediction. *Geotherm. Biol. Geochem. Yellowstone Natl. Park* 186–202.
69. Ward, D.M., M.M. Bateson, R. Weller, and A.L. Ruff-Roberts. 1992. Ribosomal RNA analysis of microorganisms as they occur in nature, p. 219–286. *In* *Advances in Microbial Ecology*. Springer, Boston, MA.
70. Ward, D.M., M.J. Ferris, S.C. Nold, and M.M. Bateson. 1998. A natural view of microbial biodiversity within hot spring cyanobacterial mat communities. *Microbiol. Mol. Biol. Rev.* 62:1353–1370.
71. Ward, L.M., J. Hemp, P.M. Shih, S.E. McGlynn, and W.W. Fischer. 2018. Evolution of phototrophy in the *Chloroflexi* phylum driven by horizontal gene transfer. *Front. Microbiol.* 9:260.
72. Wemheuer, B., R. Taube, P. Akyol, F. Wemheuer, and R. Daniel. 2013. Microbial diversity and biochemical potential encoded by thermal spring metagenomes derived from the Kamchatka Peninsula. *Archaea* 2013:136714.